LETTERS
PUBLISHED ONLINE: 13 FEBRUARY 2011 | DOI: 10.1038/NMAT2968
nature materials

Scanning tunnelling microscopy and spectroscopy of ultra-flat graphene on hexagonal boron nitride

Jiamin Xue[1], Javier Sanchez-Yamagishi[2], Danny Bulmash[2], Philippe Jacquod[1,3], Aparna Deshpande[1†], K. Watanabe[4], T. Taniguchi[4], Pablo Jarillo-Herrero[2] and Brian J. LeRoy[1*]

Graphene has demonstrated great promise for future electronics technology as well as fundamental physics applications because of its linear energy–momentum dispersion relations which cross at the Dirac point[1,2]. However, accessing the physics of the low-density region at the Dirac point has been difficult because of disorder that leaves the graphene with local microscopic electron and hole puddles[3–5]. Efforts have been made to reduce the disorder by suspending graphene, leading to fabrication challenges and delicate devices which make local spectroscopic measurements difficult[6,7]. Recently, it has been shown that placing graphene on hexagonal boron nitride (hBN) yields improved device performance[8]. Here we use scanning tunnelling microscopy to show that graphene conforms to hBN, as evidenced by the presence of Moiré patterns. However, contrary to predictions[9,10], this conformation does not lead to a sizeable band gap because of the misalignment of the lattices. Moreover, local spectroscopy measurements demonstrate that the electron–hole charge fluctuations are reduced by two orders of magnitude as compared with those on silicon oxide. This leads to charge fluctuations that are as small as in suspended graphene[6], opening up Dirac point physics to more diverse experiments.

Graphene was first isolated on silicon oxide because of the ability to image monolayer regions using an optical microscope[11]. However, the electronic properties of SiO_2 are not ideal for graphene because of the high roughness and trapped charges in the oxide. These impurity-induced charge traps tend to cause the graphene to electronically break up into electron- and hole-doped regions at low charge density, which both limit device performance and make the Dirac point physics inaccessible[3–5,12,13]. To create devices with fewer puddles, the substrate must be removed or changed. One possibility to eliminate substrate interactions is to suspend graphene[6,7], as shown by the drastic improvement in mobility which has enabled the observation of the fractional quantum Hall effect in suspended devices[14,15]. However, the freely-suspended monolayers are very delicate, leading to fabrication difficulties as well as strain[16]. Because of these difficulties, there have been no STM spectroscopy measurements of suspended graphene devices. All of this points to the need for new substrates that offer mechanical support to the graphene without interfering with its electrical properties. Recently, such a candidate substrate has been found with the demonstration of high-quality graphene devices on hexagonal boron nitride (hBN; ref. 8). Hexagonal boron nitride has the same atomic structure as graphene, but with a 1.8% longer lattice constant[17], and shares many similar properties with graphene, except that it is a wide-bandgap electric insulator[18]. The planar structure of hBN cleaves into an ultra-flat surface and the ionic bonding of hBN should leave it free of dangling bonds and charge traps at the surface. Indeed, graphene-on-hBN devices exhibit the highest mobility reported on any substrate, as well as narrow Dirac peak resistance widths, indicating reduced disorder and charge inhomogeneity[8].

To study how the local electronic structure of graphene is affected by the hBN substrate, we prepare graphene on hBN devices for STM measurements. A schematic of the measurement set-up of the graphene flake on hBN with gold electrodes for electrical contact is shown in Fig. 1a. A typical STM image of monolayer graphene showing the surface corrugations on a hBN substrate is shown in Fig. 1b. This image can be compared with an STM image of monolayer graphene prepared in a similar manner but on SiO_2 (Fig. 1c). It is clear that the surface corrugations are much larger for graphene on SiO_2 as compared to on hBN. This is because of the graphene conforming to the substrate[19] and the planar nature of hBN as compared with the amorphous SiO_2. Figure 1d shows a histogram of the heights in the two images. In both cases, the heights are well described by Gaussian distributions with standard deviations of 224.5 ± 0.9 pm for graphene on SiO_2 and 30.2 ± 0.2 pm for graphene on hBN. The values for graphene on SiO_2 are similar to previously reported[20,21], whereas the distribution for graphene on hBN is similar to graphene on mica or HOPG (ref. 22). Reducing the surface roughness is critical for graphene devices because local curvature can lead to electronic effects such as doping[23] and random effective magnetic fields[24].

Looking more closely at the topography of graphene on hBN, we resolve its atomic lattice and also observe longer periodic modulations that result in a distinct Moiré pattern (Fig. 2a,c). These two images were acquired from different areas of the same graphene flake and show different Moiré patterns resulting from a rotation of the graphene with respect to the underlying hBN lattice. In the case of Fig. 2a,c, we find long wavelength modulations of 2.6 nm and 1.3 nm respectively. By examining the Fourier transform of these images, we can learn about the underlying hBN substrate as well as its relative orientation with respect to the graphene lattice. We see two distinct sets of peaks in the FFT, there is a set of six points near the centre of the images which correspond to the Moiré pattern and there are six additional points near the edge of the images which correspond to the graphene atomic lattice. The locations of these points are rotated with respect to each other in the two images. For Fig. 2b, the atomic lattice is rotated by $12.6° \pm 1.0°$ from the horizontal. In the case of Fig. 2d, the atomic lattice is

[1]Department of Physics, University of Arizona, Tucson, Arizona 85721, USA, [2]Department of Physics, Massachusetts Institute of Technology, Cambridge, Massachusetts 02138, USA, [3]College of Optical Sciences, University of Arizona, Tucson, Arizona 85721, USA, [4]Advanced Materials Laboratory, National Institute for Materials Science, 1-1 Namiki, Tsukuba 305-0044, Japan. †Present address: Department of Materials Science and Engineering, Northwestern University, Evanston, Illinois, 60208 USA. *e-mail: leroy@physics.arizona.edu.

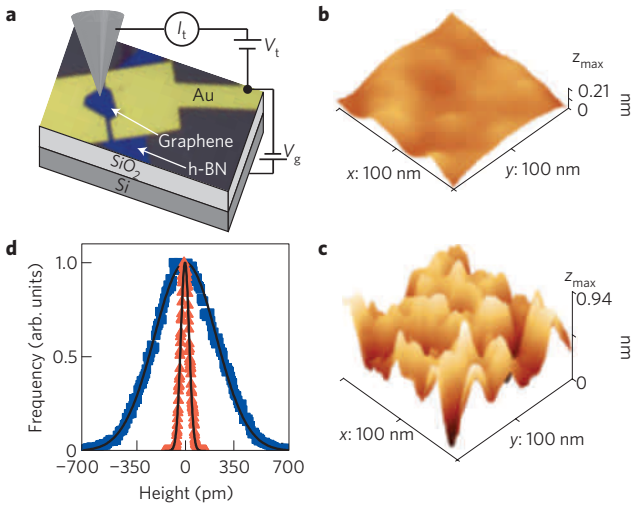

Figure 1 | Schematic device set-up and topography comparison of graphene on hBN and SiO_2. a, Optical microscope image of the mechanically exfoliated monolayer graphene flake with hBN underneath and gold electrodes contacting it above. The wiring of the STM tip and back gate voltage is indicated. **b**, STM topographic image of monolayer graphene on hBN showing the underlying surface corrugations. The image is 100 nm × 100 nm. The imaging parameters are tip voltage $V_t = -0.3$ V, tunnelling current $I_t = 100$ pA. **c**, STM topographic image of monolayer graphene on SiO_2 showing markedly increased corrugations. The imaging parameters are tip voltage $V_t = -0.5$ V, tunnelling current $I_t = 50$ pA. **d**, Histogram of the height distributions for graphene on SiO_2 (blue squares) and graphene on hBN (red triangles) along with Gaussian fits.

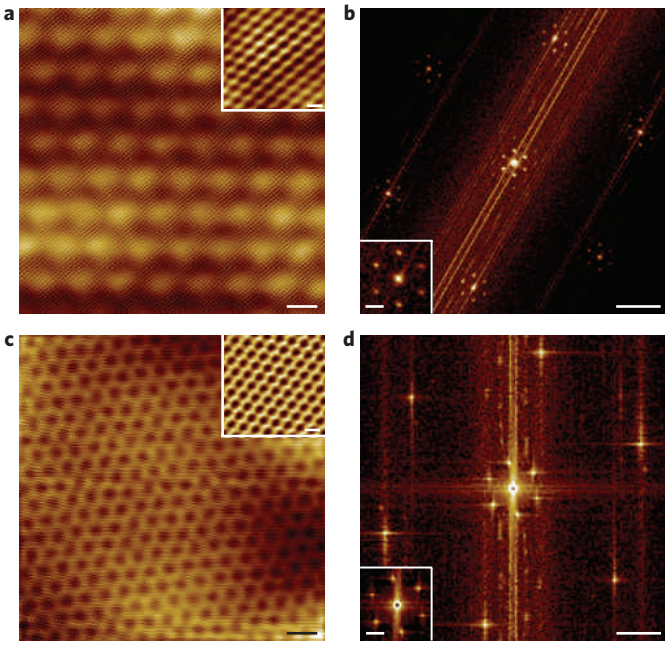

Figure 2 | Real space and Fourier transforms of Moiré patterns a, STM topographic images of a Moiré pattern produced by graphene on hBN. The scale bar is 2 nm. The inset is a zoom in of a 2 nm region with a scale bar of 0.3 nm. The imaging parameters are $V_t = -0.3$ V and $I_t = 100$ pA. **b**, Fourier transform of **a** showing the six graphene lattice points near the edge of the image and the long wavelength Moiré pattern near the centre of the image and around each lattice point. The scale bar is 10 nm^{-1}. The inset is a zoom in around one of the lattice points with a scale bar of 2 nm^{-1}. **c**, STM topographic image from another region of the same graphene flake showing a different Moiré pattern. The scale bar is 2 nm. The inset is a zoom in of a 2 nm region with a scale bar of 0.3 nm. The imaging parameters are $V_t = -0.3$ V and $I_t = 100$ pA. **d**, Fourier transform of **c** showing the atomic lattice as well as the Moiré pattern. The scale bar is 10 nm^{-1}. The inset is a zoom of the Moiré pattern with a scale bar of 4 nm^{-1}.

rotated by 18.5° ± 0.6°. In contrast the Moiré pattern is rotated by 29.9° ± 0.1° from the horizontal in Fig. 2b and 38.4° ± 0.2° from the horizontal in Fig. 2d. From the lengths of the Moiré patterns and their angles, we can calculate the orientation of the graphene lattice with respect to the underlying hBN (see Supplementary Information). In the case of Fig. 2a, we find that the hBN is rotated by −5.4° from the graphene. On the other hand, for Fig. 2c, we find that the hBN is rotated by −10.9°. This difference of 5.5° matches the difference in the orientations of the graphene lattices in the two images. Therefore, we conclude that the underlying hBN substrate is continuous and the graphene above it sits at two different angles. Atomic force microscopy images show that graphene on hBN tends to form flat regions separated by ridges and pyramids (see Supplementary Information). As the two STM images were taken from different sides of one of these ridges, it is clear that the graphene can change orientation across these ridges.

We have performed scanning tunnelling spectroscopy of the graphene on hBN. Figure 3a shows a typical dI/dV spectroscopy curve, which is proportional to the local density of states. The curve is nearly linear in energy, with a minimum near zero tip voltage indicating the energy of the Dirac point. The minimum does not go to zero, indicating the presence of some finite density of states at the Dirac point. The location of this minimum can be varied by applying a back gate voltage, V_g, to the sample. Figure 3b plots dI/dV as a function of tip voltage and gate voltage. The white line follows the minimum in the dI/dV curves for each value of the gate voltage. The white line crosses $V_t = 0.0$ at $V_g \neq 0$, indicating that there may be some residual adsorbates on the sample. This minimum occurs when the Fermi energy of the tip lines up with the Dirac point. We observe that the location of the minimum changes more quickly when the Dirac point is near zero tip voltage, which is consistent with the linear band structure of graphene. There is also a dark ridge that occurs at decreasing tip voltage as the gate voltage is increased (yellow dashed line). This is because the voltage on the tip acts as a local gate and changes the density of electrons in the graphene[25].

Our local spectroscopy measurements indicate that there is no band gap induced in graphene on hBN, not even locally. These results disagree with earlier theoretical calculations that predicted the opening of a band gap of approximately 50 meV caused by the breaking of sublattice symmetry[9,10]. This discrepancy is explained by the 1.8% mismatch between the graphene and hBN lattices and the different orientations of the two lattices, which were both neglected in refs 9,10. Taking these into account, one expects that, although one of the carbon atoms may sit over a boron (nitrogen) atom at one location, this alignment gets lost a few lattice constants away. In large enough systems, carbon atoms should therefore have the same probability to have a boron or a nitrogen atom as nearest-neighbour in the hBN layer, regardless of their sublattice index. We numerically checked the validity of this hypothesis by calculating the interlayer hopping potential $\sim\gamma_\perp \exp[-|\mathbf{r}-\mathbf{r}'|/\xi]$ from a carbon atom at $\mathbf{r}$ in the graphene layer to a boron or nitrogen atom at $\mathbf{r}'$ in a rotated hBN layer. We restricted ourselves to nearest- and next-nearest-neighbour interlayer hopping and chose the parameters $\gamma_\perp = 0.39$ eV and $\xi = 0.032$ nm to fit known values for these hoppings in graphene bilayers[26]. We found that the 1.8% lattice mismatch alone is sufficient to make the hopping strength from a carbon atom to a boron or a nitrogen atom independent of the graphene sublattice index for systems of a few hundred unit cells, going down to a few tens of unit cells when the lattices are misaligned by about one degree. We incorporated

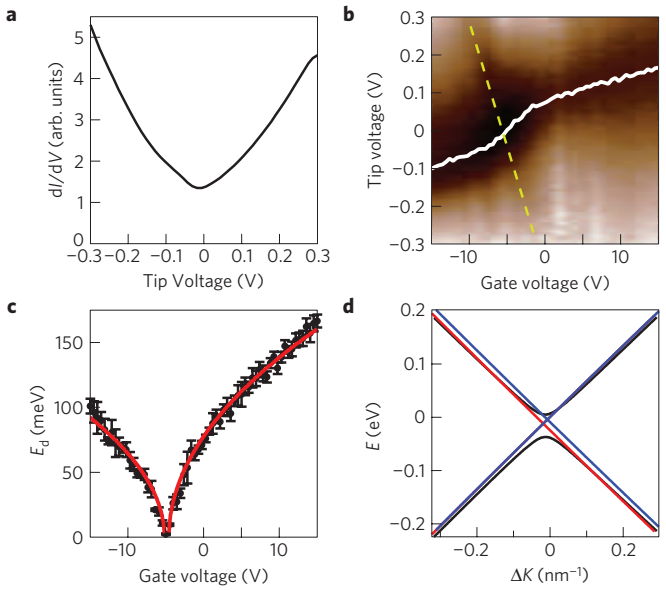

Figure 3 | Spectroscopy of graphene on hBN as a function of gate voltage. **a**, dI/dV spectroscopy showing a nearly linear density of states as a function of energy (tip voltage). **b**, dI/dV spectroscopy as a function of tip voltage and gate voltage. The white line corresponds to the minimum in the dI/dV curves and represents the Dirac point. **c**, Energy of the Dirac point as a function of gate voltage. The red curve is a fit assuming a linear band structure. **d**, Energy versus momentum dispersion relations for the case of graphene and hBN having the same lattice constant and zero angle mismatch (black curve) and two curves with 1.8% lattice mismatch. The blue curve has −5.45° angle mismatch and the red curve has −10.9°.

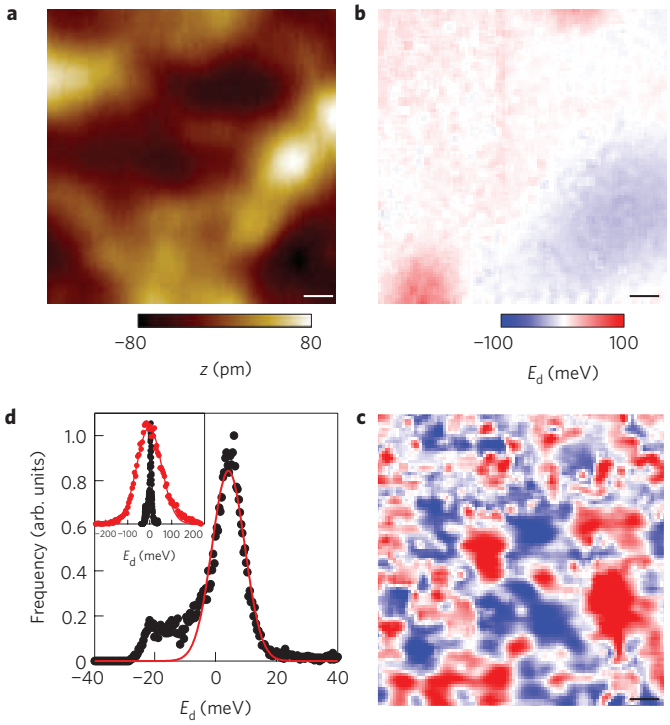

Figure 4 | Spatial maps of the density of states of graphene on hBN and SiO_2. **a**, Topography of graphene on hBN. **b**, Tip voltage at the Dirac point as a function of position for graphene on hBN. **c**, Tip voltage at the Dirac point as a function of position for graphene on SiO_2. The colour scale is the same for **b** and **c**. The scale bar in all images is 10 nm. **d** Histogram of the energies of the Dirac point from **b** as well as a Gaussian fit. The inset shows the same data but also includes the histogram for SiO_2 shown in red.

the Fourier transform of this hopping potential into the low-energy Hamiltonian for graphene on hBN to find the energy–momentum dispersion. The inter-layer coupling is nonzero only for $\mathbf{k} = 0$ as well as for six additional vectors $\mathbf{k}$ associated with the Moiré pattern. Most importantly, we found that the coupling between the A and B atoms in the graphene lattice with the boron and nitrogen atoms in the hBN are almost identical. Thus, sublattice symmetry is restored and a gapless Dirac spectrum is recovered, albeit at slightly shifted values of **K**. This is illustrated in Fig. 3d. More details of our numerical approach are given in the Supplementary Information.

By determining the energy of the Dirac point as a function of gate voltage, we can measure the Fermi velocity of electrons and holes in graphene. Figure 3c shows the energy of the Dirac point as a function of gate voltage. Graphene has a linear dispersion relation such that $E = \hbar v_F k$, where v_F is the Fermi velocity. As it is a two-dimensional material, the density of electrons is given by $n = g_s g_v \pi k^2/(2\pi)^2$, where g_s and g_v are the spin and valley degeneracies, both of which are 2. Therefore, the Dirac point should depend on gate voltage as $E = \hbar v_F \sqrt{\pi \alpha V_g}$, with α determined by the capacitance to the gate (see Methods). The red curve is a fit to the data, from which we can extract the Fermi velocity. We find that $v_F = 1.16 \pm 0.01 \times 10^6\ \mathrm{m\,s^{-1}}$ for the electrons and $v_F = 0.94 \pm 0.02 \times 10^6\ \mathrm{m\,s^{-1}}$ for the holes. Moreover, we observe an asymmetry between the Fermi velocity for electrons and holes of about 25% depending on the Moiré pattern observed. The shorter Moiré pattern has a higher Fermi velocity for holes whereas the longer one has a higher Fermi velocity for electrons. This asymmetry is larger than for graphene on SiO_2 (ref. 5) or graphene on graphite[27], which have discrepancies less than 10%. The origin of this asymmetry is unclear but it may arise as a result of next-nearest-neighbour coupling, which is not taken into account in our model.

One of the main advantages of using hBN instead of SiO_2 as a substrate for graphene is the improvement in the electronic properties of the graphene. Figure 4a shows the topography of graphene on hBN over a range of 100 nm. We have performed dI/dV measurements at 1 nm intervals over the entire area of Fig. 4a. For each of these dI/dV curves, we have found the tip voltage of the minimum, which corresponds to the Dirac point (Fig. 4b). We have done a similar analysis for a 100 nm area of graphene on SiO_2 (Fig. 4c). The red and blue regions correspond to electron and hole puddles respectively. It is clear from these two images that the variation in the energy of the Dirac point is much smaller on hBN. The spatial extent of each puddle is also much smaller in the graphene on SiO_2, consistent with an increased density of impurities[13].

We can further quantify the disorder in the graphene by looking at a histogram of the energy of the Dirac point, Fig. 4d. The main part of the histogram for the Dirac point energy on hBN is well-fitted by a Gaussian distribution (red line) with a standard deviation of 5.4 ± 0.1 meV. In addition, there is a small extra bump in the distribution from the hole-doped region near the bottom right of Fig. 4b. In comparison, the distribution on SiO_2 is much broader, with a standard deviation of 55.6 ± 0.7 meV. These distributions in energy can be converted to charge fluctuations using $n = E_d^2/\pi(\hbar v_F)^2$. We find that the charge fluctuations in graphene on hBN are $\sigma_n = 2.50 \pm 0.13 \times 10^9\ \mathrm{cm^{-2}}$, whereas they are more than 100 times larger for graphene on SiO_2, $\sigma_n = 2.64 \pm 0.07 \times 10^{11}\ \mathrm{cm^{-2}}$. Our measurements for the charge fluctuations on SiO_2 are consistent with previous single electron transistor[3] and STM (refs 4,5) measurements. Furthermore, our measurements for the charge fluctuations in graphene on hBN show a very similar value to those extracted from electrical transport measurements in suspended graphene samples[6], implying that using hBN as a substrate provides a similar benefit

to suspending graphene but without the associated fabrication challenges and limitations.

We have demonstrated that graphene on hBN provides an extremely flat surface that significantly reduces electron–hole puddles as compared to SiO_2. By reducing the charge fluctuations, the low density regime and the Dirac point can be more readily accessed. Moreover, hBN allows this low-density regime to be reached in a substrate-supported system that will allow local probe studies of the Dirac point physics with atomic resolution.

Methods

Thin and flat few layer hBN flakes were prepared by mechanical exfoliation of hBN single crystals on SiO_2/Si substrates. The hBN growth method has been previously described[28]. Exfoliated graphene flakes were then transferred to the hBN using Poly(methyl methacrylate) (PMMA) as a carrier[8] and Cr/Au electrodes were deposited using standard electron beam lithography. The lithography process leaves some PMMA resist on the surface of the graphene which is cleaned by annealing in argon and hydrogen at 350 °C for 3 h (ref. 29). The device was then immediately transferred to the STM (Omicron low-temperature STM operating at $T = 4.5$ K in an ultrahigh vacuum ($p \leq 10^{-11}$ mbar)). Electrochemically-etched tungsten tips were used for imaging and spectroscopy. All of the tips used were first checked on an Au surface to ensure that their density of states was constant.

The dI/dV spectroscopy was acquired by turning off the feedback loop and holding the tip a fixed distance above the surface. A small a.c. modulation of 5 mV at 563 Hz was applied to the tip voltage and the corresponding change in current was measured using lock-in detection. We also measured dI/dV curves with 0.5 mV excitation and observed the same results.

The voltage on the back gate induces a charge on the graphene of $n = \alpha V_g$ with $\alpha = 7.2 \times 10^{10}\ e\ \mathrm{cm}^{-2}\ \mathrm{V}^{-1}$ based on a parallel plate capacitor model. In the model, we have assumed 285 nm of SiO_2 with a dielectric constant of 3.9 and 14 nm of hBN with a dielectric constant of 3–4 (ref. 30). The thickness of the hBN was determined by atomic force microscope measurements before transferring the graphene. There is a small uncertainty in the value of α, of about 1%, due to the uncertainty in the dielectric constant of hBN.

Received 20 December 2010; accepted 19 January 2011; published online 13 February 2011

References

1. Geim, A. K. & Novoselov, K. S. The rise of graphene. *Nature Mater.* **6,** 183–191 (2007).
2. Castro Neto, A. H., Guinea, F., Peres, N. M. R., Novoselov, K. S. & Geim, A. K. The electronic properties of graphene. *Rev. Mod. Phys.* **81,** 109–162 (2009).
3. Martin, J. *et al.* Observation of electron–hole puddles in graphene using a scanning single-electron transistor. *Nature Phys.* **4,** 144–148 (2008).
4. Deshpande, A., Bao, W., Miao, F., Lau, C. N. & LeRoy, B. J. Spatially resolved spectroscopy of monolayer graphene on SiO_2. *Phys. Rev. B* **79,** 205411 (2009).
5. Zhang, Y., Brar, V. W., Girit, C., Zettl, A. & Crommie, M. F. Origin of spatial charge inhomogeneity in graphene. *Nature Phys.* **5,** 722–726 (2009).
6. Du, X., Skachko, I., Barker, A. & Andrei, E. Y. Approaching ballistic transport in suspended graphene. *Nature Nanotech.* **3,** 491–495 (2008).
7. Bolotin, K. I., Sikes, K. J., Hone, J., Stormer, H. L. & Kim, P. Temperature-dependent transport in suspended graphene. *Phys. Rev. Lett.* **101,** 096802 (2008).
8. Dean, C. R. *et al.* Boron nitride substrates for high-quality graphene electronics. *Nature Nanotech.* **5,** 722–726 (2010).
9. Giovannetti, G., Khomyakov, P. A., Brocks, G., Kelly, P. J. & van den Brink, J. Substrate-induced band gap in graphene on hexagonal boron nitride: *Ab initio* density functional calculations. *Phys. Rev. B* **76,** 073103 (2007).
10. Slawinska, J., Zasado, I. & Klusek, Z. Energy gap tuning in graphene on hexagonal boron nitride bilayer system. *Phys. Rev. B* **81,** 155433 (2010).
11. Novoselov, K. S. *et al.* Two-dimensional atomic crystals. *Proc. Natl Acad. Sci. USA* **102,** 10451–10453 (2005).
12. Chen, J-H. *et al.* Charged-impurity scattering in graphene. *Nature Phys.* **4,** 377–381 (2008).
13. Rossi, E. & Das Sarma, S. Ground state of graphene in the presence of random charged impurities. *Phys. Rev. Lett.* **101,** 166803 (2008).
14. Du, X., Skachko, I., Duerr, F., Luican, A. & Andrei, E. Y. Fractional quantum Hall effect and insulating phase of Dirac electrons in graphene. *Nature* **462,** 192–195 (2009).
15. Bolotin, K. I., Ghahari, F., Shulman, M. D., Stormer, H. L. & Kim, P. Observation of the fractional quantum Hall effect in graphene. *Nature* **462,** 196–199 (2009).
16. Bao, W. *et al.* Controlled ripple texturing of suspended graphene and ultrathin graphite membranes. *Nature Nanotech.* **4,** 562–566 (2009).
17. Liu, L., Feng, Y. P. & Shen, Z. X. Structural and electronic properties of h-BN. *Phys. Rev. B* **68,** 104102 (2003).
18. Watanabe, K., Taniguchi, T. & Kanda, H. Direct-bandgap properties and evidence for ultraviolet lasing of hexagonal boron nitride single crystal. *Nature Mater.* **3,** 404–409 (2004).
19. Cullen, W. G. *et al.* High-fidelity conformation of graphene to SiO_2 topographic features. *Phys. Rev. Lett.* **100,** 215504 (2010).
20. Ishigami, M., Chen, J. H., Cullen, W. G., Fuhrer, M. S. & Williams, E. D. Atomic structure of graphene on SiO_2. *Nano Lett.* **7,** 1643–1648 (2007).
21. Stolyarova, E. *et al.* High-resolution scanning tunnelling microscopy imaging of mesoscopic graphene sheets on an insulating surface. *Proc. Natl Acad. Sci. USA* **104,** 9209–9212 (2007).
22. Lui, C. H., Liu, L., Mak, K. F., Flynn, G. W. & Heinz, T. F. Ultraflat graphene. *Nature* **462,** 339–341 (2009).
23. Kim, E. A. & Castro Neto, A. H. Graphene as an electronic membrane. *Europhys. Lett.* **84,** 57007 (2009).
24. Guinea, F., Katsnelson, M. I. & Vozmediano, M. A. H. Midgap states and charge inhomogeneities in corrugated graphene. *Phys. Rev. B* **77,** 0705422 (2008).
25. Choudhury, S. K. & Gupta, A. K. Tip induced doping effects in local tunnel spectra of graphene. Preprint at http://arxiv.org/abs/1008.3606v1 (2010).
26. Zhang, L. M. *et al.* Determination of the electronic structure of bilayer graphene from infrared spectroscopy. *Phys. Rev. B* **78,** 235408 (2008).
27. Li, G., Luican, A. & Andrei, E. Y. Scanning tunnelling spectroscopy of graphene on graphite. *Phys. Rev. Lett.* **102,** 176804 (2009).
28. Taniguchi, T. & Watanabe, K. Synthesis of high-purity boron nitride single crystals under high pressure by using Ba–Bn solvent. *J. Cryst. Growth* **303,** 525–529 (2007).
29. Meyer, J. C. *et al.* The structure of suspended graphene sheets. *Nature* **446,** 60–63 (2007).
30. Young, A. F. *et al.* Electronic compressibility of gapped bilayer graphene. Preprint at http://arxiv.org/abs/1004.5556v2 (2010).

Acknowledgements

The authors would like to thank W. Bao, Z. Zhao and C. N. Lau for providing the graphene on SiO_2 samples used for the comparison with graphene on hBN. J.X., A.D. and B.J.L. were supported by US Army Research Laboratory and the US Army Research Office under contract/grant number W911NF-09-1-0333 and the National Science Foundation CAREER award DMR-0953784. P.J. was supported by the National Science Foundation under award DMR-0706319. J.S-Y., D.B. and P.J-H. were supported by the US Department of Energy, Office of Basic Energy Sciences, Division of Materials Sciences and Engineering under Award DE-SC0001819 and by the 2009 US Office of Naval Research Multi University Research Initiative (MURI) on Graphene Advanced Terahertz Engineering (Gate) at MIT, Harvard and Boston Unversity.

Author contributions

J.X. and B.J.L. performed the STM experiments for graphene on hBN. A.D. performed the STM experiments for graphene on SiO_2. J.S-Y. and D.B. fabricated the devices. P.J. performed the theoretical calculations. K.W. and T.T. provided the single crystal hBN. P.J-H. and B.J.L. conceived and provided advice on the experiments. All authors participated in discussing the data and writing the manuscript.

Additional information

The authors declare no competing financial interests. Supplementary information accompanies this paper on www.nature.com/naturematerials. Reprints and permissions information is available online at http://npg.nature.com/reprintsandpermissions. Correspondence and requests for materials should be addressed to B.J.L.